Analyst

RSC Publishing

PAPER

Direct analysis in real time mass spectrometry (DART-MS) of "bath salt" cathinone drug mixtures

Cite this: *Analyst*, 2013, **138**, 3424

Ashton D. Lesiak,[a] Rabi A. Musah,[a] Robert B. Cody,[b] Marek A. Domin,[c] A. John Dane[b] and Jason R. E. Shepard*[a]

Received 19th February 2013
Accepted 15th April 2013

DOI: 10.1039/c3an00360d

www.rsc.org/analyst

Rapid and versatile direct analysis in real time mass spectrometry (DART-MS) methods were developed for detection and characterization of synthetic cathinone designer drugs, also known as "bath salts". The speed and efficiency associated with DART-MS testing of such highly unpredictable samples demonstrate the technique as an attractive alternative to conventional GC-MS and LC-MS methods. A series of isobaric and closely related synthetic cathinones, alone and in mixtures, were differentiated using high mass accuracy and in-source collision induced dissociation (CID). Crime laboratories have observed a dramatic rise in the use of these substances, which has caused sample testing backlogs, particularly since the myriad of structurally related compounds are challenging to efficiently differentiate. This challenge is compounded by the perpetual emergence of new structural variants as soon as older generation derivatives become scheduled. Because of the numerous chemical substances that fall into these categories, along with the varying composition and complexity of mixtures of these drugs, DART-MS CID has the potential to dramatically streamline sample analysis, minimize the number of sample preparation steps, and enable rapid characterization of emerging structural analogs.

Introduction

The dramatic increased incidence of abuse of unregulated psychoactive substances continues to present a challenge for law enforcement agencies. The preponderance of these new designer drugs are synthetic cathinones, central nervous system stimulants with pharmacodynamic properties similar to those of amphetamines.[1–5] As their name suggests, these alkaloid derivatives are structurally related to cathinone, a natural product found in the flowering plant *Catha edulis*, commonly known as "khat".[2,3,5–7] However, the original cathinone compound has been systematically modified through nuanced structural substitutions to the parent molecule backbone, to create an extensive array of psychoactive compounds that now represents its own class of designer drugs. The core phenylethylamine backbone has multiple derivatization sites, resulting in over 100 structural analogs or related possible variants. These synthetic cathinones are marketed by various online suppliers as "bath salts" or "plant food", and are advertised as providing a "legal high" alternative to other more common, but regulated drugs of abuse.

Cathinone derivatives intended for abuse first appeared in the early to mid 2000's, and within a few years, more widespread use was reported. Cathinone abuse was subsequently followed by an increase in reports to poison control centers, and case studies suggesting dramatic yearly increases in emergency room visits.[2,5–14] While abuse of synthetic cathinones in their pure form has been documented, they are commonly formulated in combination with such substances as caffeine or lidocaine, or as mixtures of multiple cathinones.[9,12,13,15] Testing such mixtures and identifying the active components is challenging. Before regulations were enacted, these substances were widely available for sale in stores and on the internet. Post-regulation, a large number of synthetic variants and new formulations continue to emerge,[12,13,16] such that profiling of known or suspected active ingredients is still problematic, contributing to testing backlogs in the U.S.[17–21] Accordingly, manufacturers, distributors, and many drug abusers are attracted to this class of drug. As tests are developed to better screen for the presence of known synthetic cathinones, new and as yet unidentified derivatives are synthesized and distributed by manufacturers. Thus, although conventional methods that can be used to detect the presence of known cathinones are available, even more essential are rapid techniques that can facilitate determination of unknowns or enable structural elucidation of closely related substances such as isomers. Given the large number of known structural analogs, the perpetual emergence of novel derivatives, and the rapidity with which they appear on the market, appropriate instrumentation and methods that can readily identify the presence of prohibited compounds is highly desirable.

[a]*Department of Chemistry, University at Albany, State University of New York (SUNY), 1400 Washington Ave., Albany, NY 12222, USA. E-mail: jshepard@albany.edu*

[b]*JEOL USA, Inc., 11 Dearborn Rd, Peabody, MA 01960, USA*

[c]*Mass Spectrometry Center, Merkert Chemistry Center, Boston College, 2609 Beacon Street, Chestnut Hill, MA 02467-3808, USA*

The most common and widespread methods for detection and identification of drugs of abuse are electron-impact (EI) GC-MS and LC-MS, in combination with mass spectral library search results and comparisons to standards. Although these methods still represent the gold standard for routine analysis and identification of illicit drugs, the continuing emergence and increasing availability of structural variants of illegal drugs reduces their utility as tools for the identification of the rapidly increasing number of "modified" drugs, including closely related structural isomers. Challenges include the fact that (1) standards for comparison are rare or non-existent,[14] and thus, screening methods that rely on a library search for identification yield negative results even when illicit drug variants are present; and (2) the commonly observed absence of the molecular ion peak for drug classes such as amphetamines and cathinones can make compound identification challenging.[13,22–28] Some of these issues can be addressed through exploitation of newly developed instrumentation. For example, ambient mass spectrometric techniques have been applied to a wide range of forensic analyses,[9,29–32] and a number of these techniques have demonstrated promise in accommodating the high throughput capabilities that are often necessary to rapidly analyze the increasingly large influx of designer drug samples experienced by crime laboratories. Ambient MS techniques in particular have demonstrated promise in the analysis of drugs such as ecstasy and amphetamines,[33–37] cannabinoids,[38–42] and cathinones.[32,43,44] However, despite their potential to provide more detailed structural information,[36,38,45,46] few of these ambient ionization MS techniques have been applied beyond basic formula weight determinations for the analysis of designer drugs. Recent studies illustrate the significant advantages that can be gained in illicit drug identification studies from the coupling of a high mass accuracy time of flight (TOF) mass analyzer,[27,38,40,47,48] or with in-source collision-induced dissociation (CID) for promotion of molecular fragmentation.[27,36,38,45,49,50] These advantages include the ability to distinguish between closely related structural isomers, as well as the ability to detect the presence of core chemical skeletons of illicit classifications of drugs. In our efforts to extend designer drug analysis testing beyond tentative or preliminary identification, we have applied direct analysis in real time (DART)-MS methodology coupled with high mass accuracy time-of-flight (TOF) and in-source CID fragmentation to cathinone analysis. The results reported here demonstrate the broader utility of this approach in permitting differentiation of closely related compounds, including structural isomers of various cathinones both in pure form and as components of mixtures.

Experimental

DART ionization of cathinones

Positive ion mass spectra were acquired using a DART-SVP™ ion source (Ionsense, Saugus, MA, USA) interfaced to an AccuTOF mass spectrometer (JEOL USA, Inc., Peabody, MA, USA). Solid cathinone samples were sampled directly by two different methods: (a) dipping the closed end of a melting point capillary into the solid sample and positioning the sample-coated tube between the DART ion source and the detector inlet; and (b) dipping the closed end of capillary Dipit-tubes™ (Ionsense) into the solid sample and using a linear rail system to provide automated delivery of the sample to the correct sampling position between the ion source and the mass spectrometer inlet (Fig. 1).[38,51] The Dipit system is equipped with a 12-position rack that is used to hold the sampling capillary tubes. The rack is perpendicular to the ionizing gas stream and allows reproducible, automated, and optimal positioning of samples. Multiple Dipit-tubes dipped into each cathinone sample were positioned ~0.9 cm apart in the rack and transported through the helium stream laterally at a speed of 1.0 mm s^{-1} while acquiring spectra.

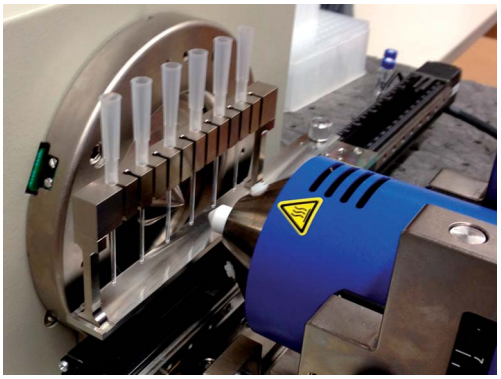

Fig. 1 The Dipit-tube linear rail system used to position sampling tubes. For analysis, the closed end of a melting point capillary tube was dipped into the individual cathinone or cathinone mixture (both solids), and placed into the rail system. The automated sampling platform allows for precise positioning of the sample tubes between the ionizing gas source (blue cylinder on right) and the mass spectrometer inlet (silver cone on left), and reduces the variation associated with manual sampling.

DART-MS parameters

An AccuTOF time-of-flight (TOF) mass spectrometer was operated in positive ion mode for all mass measurements. The resolving power of the spectrometer was 6000 (FWHM definition), measured for protonated reserpine. A mass spectrum of poly(ethylene glycol) (PEG; Sigma, St. Louis, MO, USA) with average molecular weight 600 was obtained with each data acquisition set as a reference standard to enable exact mass measurements. The atmospheric pressure interface was typically operated at the following potentials: orifice 1 was varied from 20 to 90 V, orifice 2 = 5 V, and ring lens = 3 V. The RF ion guide voltage was generally set to 500 V to allow detection of ions greater than m/z 50. All measurements fell within the instrumentation specification of ±5 mmu mass accuracy. The DART ion source was operated with helium gas (Airgas, Cambridge, MA, USA) at 350 °C, at a flow rate of 2 L min^{-1}, and a grid voltage of 530 V. TSSPro3 software (Shrader Analytical, Detroit, MI, USA) together with Mass Spec Tools programs (ChemSW Inc., Fairfield, CA, USA) were used for data processing.

GC-MS parameters

An HP 6890 series gas chromatograph equipped with an HP-5 30 m × 0.25 mm × 0.25 μL analytical column and helium as a

carrier gas (1.0 mL min^{-1}; constant flow mode) was employed. The temperature was held at 80 °C for 2 min, ramped at 15 °C min^{-1} to 280 °C, and then held for 2 min. The GC was coupled to an HP 5972A selective mass detector in electron ionization (EI) mode at 70 eV. The transfer line was set at 285 °C. The acquisition range was *m/z* 30–600.

Synthetic cathinones

All synthetic cathinones were purchased from Cayman Chemical (Ann Arbor, MI, USA). For samples comprised of cathinone mixtures, the cathinones were present in approximately equal proportions by mass.

Results and discussion

The DART ionization process has been extensively described previously,[30,52] as a soft ionization technique based on the atmospheric pressure interactions between long-lived electronic excited state helium atoms and the thermally desorbed sample. While the basic ionization process results in simple mass spectra dominated by $[M + H]^+$ species, the electrode voltage at the instrument's inlet cone can be increased to induce fragmentation. A software acquisition method termed functional switching was employed during sample analysis. This process entails changing the spectrum acquisition parameters over the course of a single analysis.[36,38,45,49,50,53] In this case, measurements were made while varying the electrode voltage from 20 V, 30 V, 60 V, and 90 V. This enabled the acquisition of both simple low voltage spectra characterized by the presence of only parent ion peaks (low voltages), and in-source CID spectra (high voltages) that exhibited fragmentation, the extent of which was dependent upon the magnitude of the electrode voltage. It has been shown previously that 90 V conditions are optimal for differentiation of synthetic cannabinoids.[38] However, under 90 V conditions, the cathinones were excessively fragmented, which in effect, lessened the differences between spectra that were essential to distinguishing one compound from another (data not shown). Ultimately, the 60 V CID spectra were found to be most informative for the differentiation of closely related cathinone species, and this voltage was determined as optimal for structural interpretation purposes. Thus, the term "CID spectra" refers to spectra obtained with the electrode voltage set at 60 V, whereas the term "non-CID spectra" refers to spectra obtained when the electrode voltage was set at 20 V. Under these latter conditions, little to no fragmentation occurred, and the spectra were dominated by the parent $[M + H]^+$ peak.

The cathinones tested herein have either been detected in seized designer drug samples or are close structural variants of such substances.[13,15,22,28,54] Two pairs of isomers were identified alone, or as components of mixtures of up to four cathinones. Table 1 shows the high mass accuracy data for all the analyzed cathinones under DART-MS CID conditions. The tabulated data shows the parent $[M + H]^+$ peak as well as a series of product ion fragment peaks that were critical in the chemical analysis of mixtures. Strikingly, although many of the non-isomeric cathinones studied have different formula weights, substantial similarity exists in the fragmentation patterns observed for these compounds, such that common fragments are lost across this family of designer drugs (highlighted in color in Table 1). For example, CID fragmentation spectra show all seven cathinones exhibited the loss of water (*m/z* 18), while six cathinones exhibited a loss of $C_4H_{11}N$ (*m/z* 73), and five of the seven cathinones showed either a loss of CH_5O, C_2H_6O, or both (*m/z* 33 and 46 respectively). Such fragments, fragmentation patterns, and their relative abundances, would presumably be critical in the structural analysis of unknowns. DART-MS spectra of the synthetic cathinones 2-ethylethcathinone and diethylcathinone are shown in Fig. 2. Fig. 2a and b show the CID spectra of the pure compounds, while Fig. 2c and d are mixtures of the two compounds shown as a non-CID spectrum and a CID spectrum respectively. The CID spectra of the individual cathinones are characterized by the presence of several dominant and characteristic peaks, as well as the parent $[M + H]^+$. The *m/z* values and relative abundances of the peaks that are prominent and/or unique to each cathinone are delineated in Table 2. These spectra illustrate the advantage to being able to control the extent of fragmentation with DART-MS CID. Simple GC-MS spectra of members of this family are of limited utility, as they are extensively fragmented, often do not show an appreciable parent peak, and have few peaks of any significant abundance other than common α-cleavage derived amino fragments. An example of this effect is shown in Fig. 3, where 2-ethylethcathione analyzed by GC-MS is shown. In this case, no parent peak is observable. With the exception of fragments at *m/z* 72 and 44 which are common amine fragments found in many of the cathinones (data not shown), only low abundance peaks are observed. In contrast, examination of the DART-MS CID data permits identification of fragments that can be used to demonstrate the presence of each of the two compounds, particularly as components of a mixture. Both compounds have in common the core β-ketophenethylamine structure characteristic of cathinones, and are in fact isobars, having the same formula weight. Thus, it is not apparent when a mixture of the two compounds is analyzed under non-CID conditions, whether both or only a single isomer is present (Fig. 2c). However, the CID spectra are very informative, and the relative simplicity of the cathinone structures results in CID fragmentation that is quite predictable (Table 1). First, a series of consensus peaks appear due to cleavages resulting in charge retention on the aryl fragments, in particular the phenylethyl and tropilium ions at *m/z* 105 ($C_8H_9^+$) and 91 ($C_7H_7^+$) respectively. The mode of fragmentation of the β-ketoamine substituents also mirror each other for these two compounds, with the appearance of common fragments including product ion peaks at *m/z* 188, 160, 133, and 105, representing the loss of *m/z* 18 (H_2O), 46 (C_2H_6O), 73 ($C_4H_{11}N$) and 101 ($C_5H_{11}NO$) respectively. However, despite the overwhelming similarities, a few unique differences are also apparent that aid in their differentiation, most notably *m/z* 100 for diethylcathinone and *m/z* 173 for ethylethcathinone (loss of CH_5O). Both peaks are apparent in the CID spectrum of the mixture of the two substances

Table 1 Data generated from the cathinone spectra highlighting in each case, the $[M + H]^+$ peak, the product ion peaks, and their relative abundances. Common mass losses are also included to illustrate fragmentation pathway similarities. For ease of visualization, color-coded shading corresponding to consensus loss fragments are also shown. For example, blue shading is indicative of fragments formed from the loss of H_2O from the indicated molecular ion peaks

Cathinone	Formula	Calculated	Measured (*m*/*z*)	Difference	Diff (mmu)	Relative abundance	Measured loss	Fragment lost
2-Ethylethcathinone	$C_{13}H_{20}NO$	206.1544	$[M+H]^+$ 206.1512	0.0032	3.2	82.5	—	—
	$C_{13}H_{19}N$	188.1439	188.1435	0.0004	0.4	100.0	18.0115	H_2O
	$C_{12}H_{15}N$	173.1204	173.1195	0.0009	0.9	1.7	33.0317	CH_5O
	$C_{11}H_{14}N$	160.1126	160.1118	0.0008	0.8	40.3	46.0418	C_2H_6O
	$C_7H_7N_3$	133.0640	133.0666	−0.0026	−2.6	3.5	73.0904	$C_4H_{11}N$
	C_8H_9	105.0704	105.0703	0.0001	0.1	1.5	101.0840	$C_5H_{11}NO$
	C_7H_7	91.0548	91.0551	−0.0003	−0.3	0.9	115.0996	$C_6H_{13}NO$
	$C_4H_{10}N$	72.0813	72.0763	0.0050	5.0	10.3	134.0731	$C_9H_{10}O$
Diethylcathinone	$C_{13}H_{20}NO$	206.1544	$[M+H]^+$ 206.15	0.0044	4.4	100.0	—	—
	$C_{13}H_{19}N$	188.1439	188.1449	−0.0010	−1.0	1.5	18.0119	H_2O
	$C_{11}H_{14}N$	160.1126	160.1112	0.0014	1.4	5.4	46.0398	C_2H_6O
	C_9H_9O	133.0653	133.0647	0.0006	0.6	63.5	73.0877	$C_4H_{11}N$
	C_8H_9	105.0704	105.0695	0.0009	0.9	37.0	101.0830	$C_5H_{11}NO$
	$C_6H_{14}N$	100.1126	100.1128	−0.0002	−0.2	48.8	106.0394	C_7H_6O
	C_7H_7	91.0548	91.0526	0.0022	2.2	0.9	115.0996	$C_6H_{13}NO$
	$C_4H_{10}N$	72.0813	72.0779	0.0034	3.4	30.8	134.0721	$C_9H_{10}O$
Isopentedrone	$C_{12}H_{18}NO$	192.1388	$[M+H]^+$ 192.1385	0.0003	0.3	99.0	—	—
	$C_{12}H_{16}N$	174.1283	174.1279	0.0004	0.4	92.6	18.0095	H_2O
	$C_{11}H_{13}O$	161.0966	161.0958	0.0008	0.8	100.0	31.0413	CH_5N
	$C_9H_{10}N$	132.0813	132.0808	0.0005	0.5	22.1	60.0561	C_3H_8O
	C_8H_7O	119.0497	119.0489	0.0008	0.8	16.1	73.0879	$C_4H_{11}N$
	C_7H_7	91.0548	91.0525	0.0023	2.3	98.1	101.0840	$C_5H_{11}NO$
3-Methylethcathinone	$C_{12}H_{18}NO$	192.1388	$[M+H]^+$ 192.1373	0.0015	1.5	61.8	—	—
	$C_{12}H_{16}N$	174.1283	174.1243	0.0040	4.0	100.0	18.0099	H_2O
	$C_{11}H_{13}N$	159.1048	159.1051	−0.0003	−0.3	10.8	33.0344	CH_5O
	$C_{10}H_{12}N$	146.0970	146.0962	0.0008	0.8	51.7	47.0493	C_2H_7O
	C_9H_9N	131.0735	131.0772	−0.0037	−3.7	3.4	61.0642	C_3H_9O
	C_9H_{11}	119.0871	119.0878	−0.0007	−0.7	12.1	73.0529	C_3H_7NO
	C_8H_9	105.0704	105.0704	0.0000	0.0	0.8	87.0684	C_4H_9NO
	C_7H_7	91.0548	91.0570	−0.0022	−2.2	1.1	101.0840	$C_5H_{11}NO$
	$C_4H_{10}N$	72.0813	72.0791	0.0022	2.2	1.7	120.0582	C_8H_8O
2-Methylethcathinone	$C_{12}H_{18}NO$	192.1388	$[M+H]^+$ 192.1372	0.0016	1.6	85.3	—	—
	$C_{12}H_{16}N$	174.1283	174.1243	0.0040	4.0	100.0	18.0099	H_2O
	$C_{11}H_{13}N$	159.1048	159.1051	−0.0003	−0.3	11.8	33.0344	CH_5O
	$C_{10}H_{12}N$	146.0970	146.0962	0.0008	0.8	60.8	47.0493	C_2H_7O
	C_9H_9N	131.0735	131.0772	−0.0037	−3.7	2.9	61.0642	C_3H_9O
	C_9H_{11}	119.0871	119.0878	−0.0007	−0.7	11.3	73.0529	C_3H_7NO
	C_8H_9	105.0704	105.0718	−0.0014	−1.4	0.9	87.0670	C_4H_9NO
	C_7H_7	91.0548	91.0570	−0.0022	−2.2	1.9	101.0840	$C_5H_{11}NO$
	$C_4H_{10}N$	72.0813	72.0791	0.0022	2.2	14.2	120.0581	C_8H_8O
2-Fluoromethcathinone	$C_{10}H_{13}FNO$	182.0981	$[M+H]^+$ 182.0993	−0.0012	−1.2	40.3	—	—
	$C_{10}H_{12}O_2$	164.0837	164.0848	−0.0011	−1.1	100.0	18.0145	H_2O
	C_9H_8FN	149.0640	149.0653	−0.0012	−1.2	66.5	33.0340	CH_5O
	C_8H_9FN	138.0791	138.0717	0.0002	0.2	2.3	44.0276	C_2H_4O
	C_8H_8F	123.0610	123.0594	0.0016	1.6	25.0	59.0399	C_2H_5NO
	C_8H_7	103.0548	103.0558	−0.0010	−1.0	4.8	79.0435	C_2H_6FNO
2-Fluoroethcathinone	$C_{11}H_{15}FNO$	196.1138	$[M+H]^+$ 196.1122	0.0016	1.6	45.5	—	—
	$C_{11}H_{13}FN$	178.1032	178.1024	0.0008	0.8	100.0	18.0098	H_2O
	$C_{10}H_{10}FN$	163.0797	163.0801	−0.0004	−0.4	6.5	33.0321	CH_5O
	C_9H_9FN	150.0719	150.0718	0.0001	0.1	75.0	46.0404	C_2H_6O
	C_8H_6FN	135.0484	135.0528	−0.0044	−4.4	7.8	61.0594	C_3H_9O
	C_8H_8F	123.0610	123.0594	0.0016	1.6	27.7	73.0528	C_3H_7NO

(Fig. 2d), indicating the presence of each. Additionally, in the spectrum of the mixture, the four dominant peaks for diethylcathinone (at *m*/*z* 133, 105, 100, and 72) as well as the two dominant peaks for 2-ethylcathinone (at *m*/*z* 188 and 160) are all readily apparent and dominant, an observation which also served to corroborate the presence of both in the mixture.

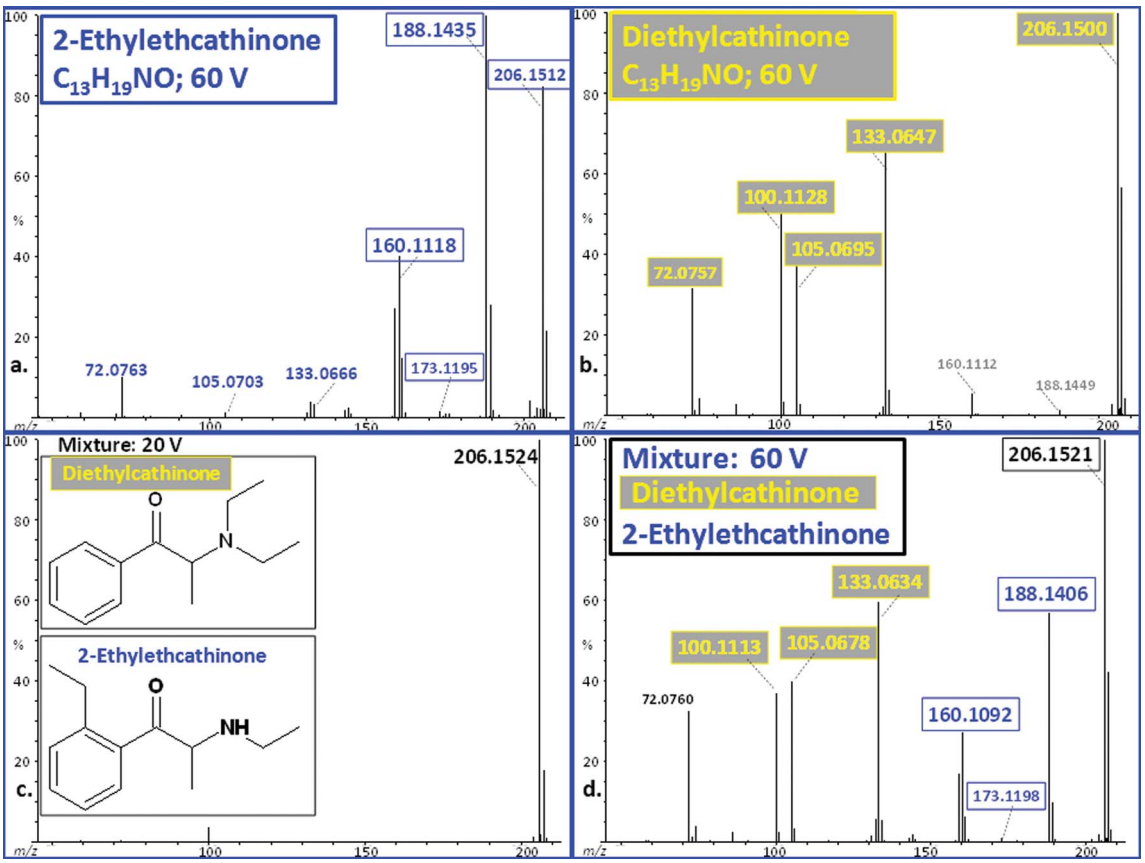

Fig. 2 DART-MS spectra of individual cathinones and a cathinone mixture. Panel a: in-source CID spectrum of 2-ethylethcathinone; Panel b: in-source CID spectrum of diethylcathinone; Panel c: spectrum of a 50/50 mixture of the two cathinones; Panel d: DART-MS in-source CID spectrum of a 50/50 mixture of the two cathinones. For both compounds, the $[M+H]^+$ peak was readily apparent. The masses representative of key product ions that were identified within the mass spectra of the individual compounds or the compound mixture are enclosed in color-coded boxes (yellow for diethylcathinone and blue for 2-ethylethcathinone). The spectral data are shown in Table 2.

Table 2 CID data used to identify the two cathinones in the mixture whose spectrum is shown in Fig. 2d. Entries highlighted in color indicate masses unique to the indicated cathinone, and the observation of which supported the presence of that particular cathinone in the mixture[a]

Mixture		2-Ethylethcathinone		Diethylcathinone	
Measured (*m*/*z*)	Abundance	Measured (*m*/*z*)	Abundance	Measured (*m*/*z*)	Abundance
100.1113	37.2	—	—	100.1128	49.2
101.1141	2.7	—	—	101.1136	3.4
105.0678	40.2	105.0703	1.6	105.0695	36.9
133.0634	59.8	133.0666	3.6	133.0647	64.0
134.0680	5.7	—	—	134.0671	6.3
160.1092	27.3	160.1118	40.2	160.1112	5.4
161.1009	6.6	161.0996	15.1	—	—
173.1180	1.2	173.1199	1.7	173.1201	0.2
188.1406	56.9	188.1435	100.0	188.1449	1.4

[a] Differences in relative abundance values for peaks that appear in both the spectrum of the pure cathinones as well as in the mixture, are a consequence of differences between desorption and ionization of the pure substance *versus* that of the mixture.

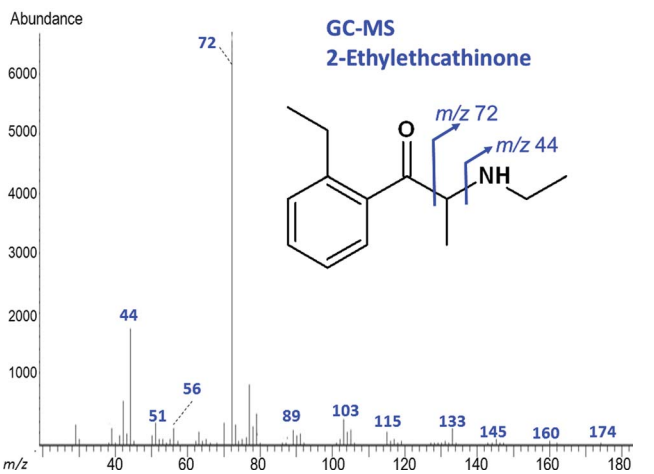

Fig. 3 GC-MS spectrum of 2-ethylethcathinone (in contrast to the DART-MS in-source CID spectrum shown in Fig. 2).

The DART-MS CID spectra of the two cathinone isomers isopentedrone and 3-methylethcathinone are shown in Fig. 4a and b. Fig. 4c and d are spectra of a mixture of the two compounds under non-CID and CID conditions respectively. To ease comparison, the data associated with the spectra presented in Fig. 4 are presented in Table 3. The 3-methylethcathinone has the classic β-ketophenethylamine backbone, while isopentedrone is a structural analog of pentedrone with the α-propyl and β-keto groups interchanged. Although these two cathinones are indistinguishable using high mass accuracy

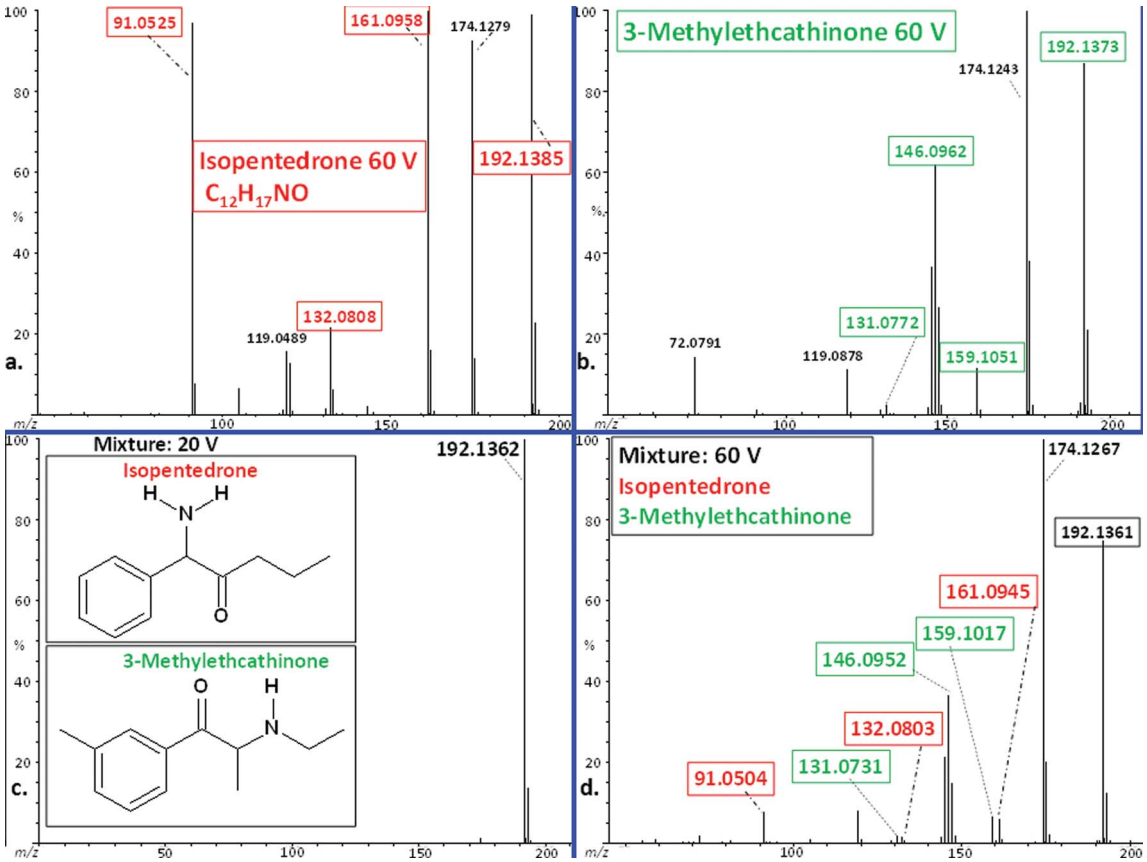

Fig. 4 DART-MS spectra of individual cathinones and a cathinone mixture. Panel a: in-source CID spectrum of isopentedrone; Panel b: in-source CID spectrum of 3-methylethcathinone; Panel c: spectrum of a 50/50 mixture of the two cathinones; Panel d: DART-MS in-source CID spectrum of a 50/50 mixture of the two cathinones. For both compounds, the $[M + H]^+$ peak was readily apparent. The masses representative of key product ions that were identified within the mass spectra of the individual compounds or the compound mixture are enclosed in color-coded boxes (green for 3-methylethcathinone and red for isopentedrone). Masses identified in black represent peaks common to both cathinones. The statistics associated with the raw spectral data are shown in Table 3.

Table 3 CID data used to identify the two cathinones in the mixture whose spectrum is shown in Fig. 4d. Entries highlighted in color indicate masses unique to the indicated cathinone, and the observation of which supported the presence of that particular cathinone in the mixture[a]

Mixture		3-Methylethcathinone		Isopentedrone	
Measured (*m*/*z*)	Abundance	Measured (*m*/*z*)	Abundance	Measured (*m*/*z*)	Abundance
91.0504	8.1	91.0526	1.1	91.0525	97.7
132.0803	1.8	132.0818	0.6	132.0807	22.0
146.0952	36.8	146.0970	51.7	146.0969	0.3
147.0817	15.2	147.0867	16.8	147.0985	0.2
159.1017	6.8	159.1035	10.8	159.1063	0.6
160.0967	1.1	160.1095	1.5	160.1030	0.2
161.0945	6.3	161.1097	0.2	161.0958	100.0

[a] Differences in relative abundance values for peaks that appear in both the spectrum of the pure cathinones as well as in the mixture, are a consequence of differences between desorption and ionization of the pure substance *versus* that of the mixture.

measurements alone, several unique and/or dominant peaks appear for each under CID conditions. These include peaks at *m*/*z* 91, 132, and 161 for isopentedrone, and peaks at *m*/*z* 131, 146, and 159 for 3-methylethcathinone. The presence of these fragments enables differentiation of the pure compounds and identification of each compound in the mixture.

"Bath salt" designer drugs have been identified as mixtures containing up to four different synthetic cathinones or other diluents, such as caffeine, lidocaine, and benzocaine.[9,13,15] Accordingly, a mixture of 2-fluoromethcathinone (2-FMC), 2-methylethcathinone (2-MEC), 2-fluoroethcathinone (2-FEC), and 2-ethylethcathinone (2-EEC) was analyzed. All four compounds have the classic β-ketophenethylamine backbone associated with cathinones, but differ based on various substituents on the aromatic ring or the length of the *N*-alkyl chain. The selection of four synthetic cathinones with different formula weights enabled us to study whether the number of compounds in a mixture could be determined under non-CID conditions, and whether the individual cathinones could be further characterized despite fragmentation of all four compounds. The non-CID DART-MS spectrum of the four-component mixture is shown in Fig. 5, with the four $[M + H]^+$ peaks indicated. The high mass accuracy CID spectra of the four pure cathinones are shown in Fig. 6 with unique masses highlighted. The CID spectrum of a mixture of all four compounds is shown in Fig. 7. Most notably, all four spectra in Fig. 6 exhibit a base peak due to loss of water. In the mixture, the $[M + H]^+$ peaks and the peaks associated with the loss of water are identified for each substance (Fig. 7). For three of the four

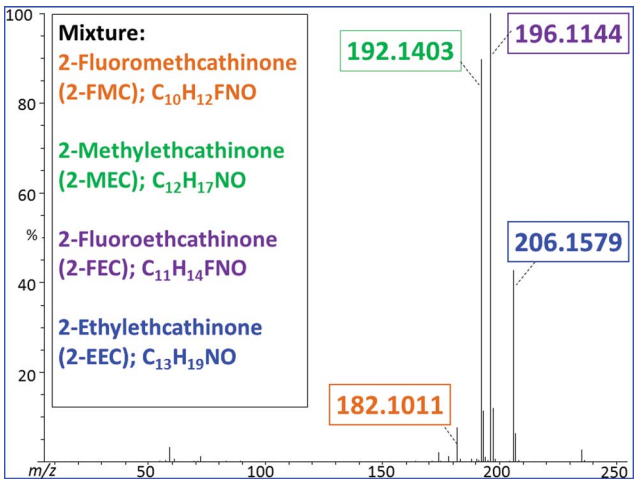

Fig. 5 DART-MS spectrum of a four synthetic cathinone mixture. The cathinone names appear in colored fonts that match the coloring of their corresponding $[M + H]^+$ masses. The CID spectra of the individual cathinones are shown in Fig. 6. The in-source CID mass spectrum of this mixture is shown in Fig. 7.

synthetic cathinones, other unique peaks were also observed in the spectrum of the mixture, such as those representing the fragment formed from the loss of C_2H_6O. This loss was observed in 2-MEC (*m*/*z* 146), 2-FEC (*m*/*z* 150), and 2-EEC (*m*/*z* 160). On the other hand, because of the structural similarity and the combination of a significant number of fragments, many other product ion peaks overlap and cannot be attributed to a single cathinone. Examples of these unattributed peaks include those at *m*/*z* 123 due to the loss of C_2H_5NO in 2-FMC and 2-FEC, and those at *m*/*z* 105, 91, and 72, which are found in both 2-MEC and 2-EEC.

Although fragment ions are useful for structure identification purposes in low resolving-power-MS experiments, extensive fragmentation can also complicate the mass spectrum, as high levels of fragmentation can impede the ability to distinguish between closely related structures due to fragmentation pattern similarities. The functional switching program allowed a series of spectra to be produced for each sample under varied conditions, essentially enabling the selection of the appropriate level of fragmentation necessary for characterizing the synthetic cathinone mixtures. Numerous isomers are known to exist within the cathinone family, and some of these structures, such as *ortho*-, *meta*-, and *para*-substituted analogs, would be challenging to discern without the use of a technique like NMR, because closely related compounds are likely to fragment in a similar, if not identical fashion. Synthetic cathinones are commonly distributed in solid form as powders, tablets and/or capsules. Importantly, although solid synthetic cathinones are most often in the salt form, these salts can be

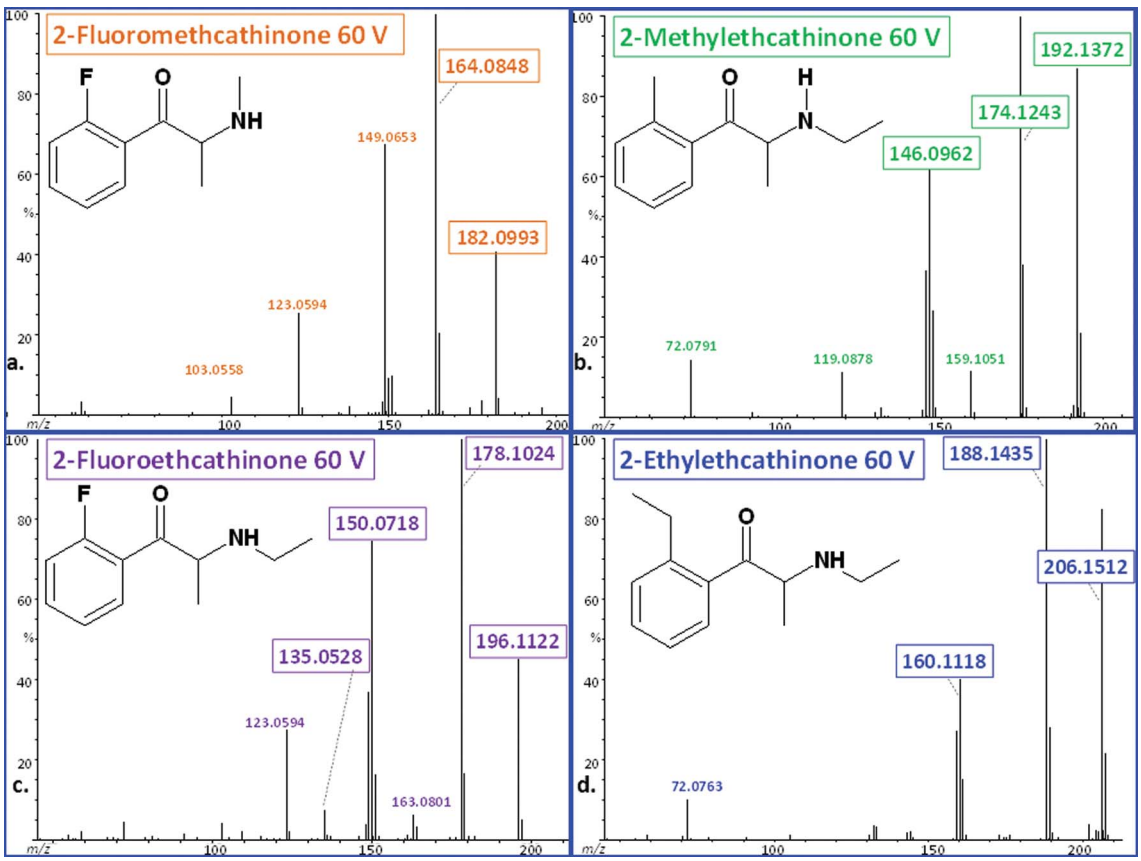

Fig. 6 DART-MS in-source CID spectra of four synthetic cathinones showing key observed fragments. The statistics associated with these data are shown in Table 1. In each case, the $[M + H]^+$ peak is readily apparent. The masses associated with key product ion peaks that were also observed in the mass spectrum of a mixture of the four compounds (see Fig. 7) are enclosed in boxes.

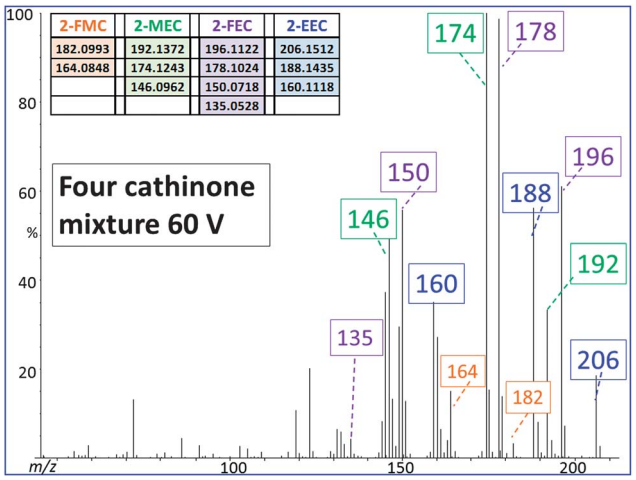

Fig. 7 DART-MS in-source CID spectrum of a four synthetic cathinone mixture. The cathinone names are abbreviated as 2-fluoromethcathinone (2-FMC), 2-methylethcathinone (2-MEC), 2-fluoroethcathinone (2-FEC), and 2-ethylethcathinone (2-EEC). The in-source CID spectra of the individual cathinones of which the mixture is comprised appear in Fig. 6. The unit masses of fragment ions unique to each cathinone that are important in facilitating identification of each cathinone in the mixture are shown in color-coded boxes, with the high mass accuracy values included in the inset. The data associated with the observed peaks are listed in Table 4.

Table 4 CID data used to identify the four cathinones in the mixture whose spectrum is shown in Fig. 6. Entries highlighted in color indicate masses unique to the indicated cathinone, and the observation of which supported the presence of that particular cathinone in the mixture[a]

2-FMC		2-FEC		2-EEC		2-MEC		Mixture	
Measured (*m/z*)	Abundance	Measured (*m/z*)	Abundance	Measured (*m/z*)	Abundance	Measured (*m/z*)	Abundance	Measured (*m/z*)	Abundance
135.0570	0.8	135.0528	7.8	-	-	-	-	135.0557	4.6
146.0982	1.0	-	-	146.0968	0.4	146.0962	62.0	146.0950	49.3
150.0683	9.5	150.0718	74.7	-	-	-	-	150.0716	55.9
-	-	-	-	160.1118	40.3	160.1079	1.5	160.1108	27.4
164.0848	100.0	164.0871	3.2	-	-	-	-	164.0871	15.2
174.1282	2.0	174.1252	0.8	174.1261	0.8	174.1243	100.0	174.1283	100.0
178.1024	3.9	178.1024	100.0	-	-	-	-	178.1023	98.8
182.0993	40.8	182.0965	1.1	-	-	-	-	182.0997	3.4
188.1444	0.8	188.1443	0.3	188.1435	100.0	188.1263	0.6	188.1438	56.4
192.1386	1.1	192.1386	0.4	192.1408	0.9	193.1372	87.1	192.1382	33.5
196.1124	2.0	196.1122	45.5	-	-	-	-	196.1122	61.2
206.1483	0.7	206.1566	0.2	206.1512	82.2	206.1534	0.9	206.1552	18.7

[a] Differences in relative abundance values for peaks that appear in both the spectrum of the pure cathinones as well as in the mixture, are a consequence of differences between desorption and ionization of the pure substance *versus* that of the mixture.

analyzed directly by DART-MS, without any sample preparation, resulting in spectra of the protonated free base. Conventional GC-MS analysis generally requires substantial sample pre-preprocessing and extraction, adding substantial time to the assay. For drug mixtures, both the drug(s) of interest and any adulterant or diluting substance could potentially be analyzed by DART-MS as described here. In CID studies, ionization and fragmentation of adulterants would add greater complexity to the identification of unknowns, but would be possible and informative in and of itself. Ultimately, to the best of our knowledge, no mixtures of greater than four components have been reported.

Conclusion

Simultaneous differentiation of multiple designer drugs of interest was performed with DART-MS. The individual components of a series of mixtures could be differentiated, including isobaric species and assorted combinations of drugs. The technique demonstrated higher throughput than is generally possible with GC-MS, and no solvents, extractions, or sample preparation whatsoever was required. Introduction of the sample to the open air space between the DART ion source and the mass spectrometer inlet yielded spectra in a few seconds. The instrument parameters described here resulted in extremely rapid analyses with no carry over between samples. High mass accuracy, a high level of versatility in comparison to other conventional forms of MS analysis, and a dramatic reduction in the time associated with analysis of complex samples was demonstrated. As emergency care providers and law enforcement organizations continue to be challenged to quickly respond to the rapid evolution of designer drugs and the consequent testing backlogs that develop, effective analytical methods such as DART-MS can provide a rapid screening alternative with minimal assay development efforts.

Acknowledgements

The authors thank the University at Albany, State University of New York, U.S.A. for financial support.

References

1 R. A. Glennon and S. M. Liebowitz, *J. Med. Chem.*, 1982, **25**, 393–397.
2 J. M. Prosser and L. S. Nelson, *J. Med. Toxicol.*, 2011, **8**, 33–42.
3 T. A. Dal Cason, *Forensic Sci. Int.*, 1997, **87**, 9–53.
4 United State Drug Enforcement Agency, *Drugs of Abuse Fact Sheet*, U.S. Department of Justice, Drug Enforcement Administration, 2011.
5 H. Belhadj-Tahar and N. Sadeg, *Forensic Sci. Int.*, 2005, **153**, 99–101.
6 J. P. Kelly, *Drug Test. Anal.*, 2011, **3**, 439–453.
7 C. Rosenbaum, S. Carreiro and K. Babu, *J. Med. Toxicol.*, 2012, **8**, 15–32.
8 A. Al-Motarreb, K. Baker and K. J. Broadley, *Phytother. Res.*, 2002, **16**, 403–413.
9 H. A. Spiller, M. L. Ryan, R. G. Weston and J. Jansen, *Clin. Toxicol.*, 2011, **49**, 499–505.
10 L. Lindsay and M. L. White, *Clin. Pediatr. Emerg. Med.*, 2012, **13**, 283–291.
11 L. Karila and M. Reynaud, *Drug Test. Anal.*, 2011, **3**, 552–559.
12 S. D. Brandt, S. Freeman, H. R. Sumnall, F. Measham and J. Cole, *Drug Test. Anal.*, 2011, **3**, 569–575.
13 S. D. Brandt, H. R. Sumnall, F. Measham and J. Cole, *Drug Test. Anal.*, 2010, **2**, 377–382.
14 S. Davis, K. Rands-Trevor, S. Boyd and M. Edirisinghe, *Forensic Sci. Int.*, 2012, **217**, 139–145.

15 S. Davies, D. M. Wood, G. Smith, J. Button, J. Ramsey, R. Archer, D. W. Holt and P. I. Dargan, *QJM*, 2010, **103**, 489–493.
16 R. Kikura-Hanajiri, N. Uchiyama and Y. Goda, *Leg. Med.*, 2011, **13**, 109–115.
17 T. Plohetski, Crime lab backlogs weighing down court system, http://www.statesman.com/news/news/local/crime-lab-backlogs-weighing-down-court-system/nWDm6/, accessed on 2/19/2013.
18 J. Kenyon, Are crime labs ready for new state crackdown on bath salts?, http://www.cnycentral.com/news/story.aspx?id=786023, accessed on 2/19/2013.
19 C. Traynor and J. Cleaver, in *Oneida Dispatch*, 2012.
20 Syracuse Post-Standard, *Oneida City Police continue to wait for bath salts test results from backlogged Albany Crime lab*, Madison Neighbors Today, http://www.syracuse.com/news/index.ssf/2012/08/oneida_city_police_continue_to.html, accessed on 2/18/2013.
21 J. Gamm, Emerson discusses bath salts with area law enforcement personnel, http://www.semissourian.com/story/1866546.html, accessed on 2/18/2013.
22 R. P. Archer, *Forensic Sci. Int.*, 2009, **185**, 10–20.
23 Y. F. H. Abiedalla, K. Abdel-Hay, J. DeRuiter and C. R. Clark, *Forensic Sci. Int.*, 2012, **223**, 189–197.
24 O. Locos and D. Reynolds, *J. Forensic Sci.*, 2012, **57**, 1303–1306.
25 D. Zuba, *TrAC, Trends Anal. Chem.*, 2012, **32**, 15–30.
26 C. R. Maheux and C. R. Copeland, *Drug Test. Anal.*, 2012, **4**, 17–23.
27 J. D. Power, S. D. McDermott, B. Talbot, J. E. O'Brien and P. Kavanagh, *Rapid Commun. Mass Spectrom.*, 2012, **26**, 2601–2611.
28 F. Westphal, T. Junge, U. Girreser, W. Greibl and C. Doering, *J. Forensic Sci.*, 2012, **217**, 157–167.
29 G. J. Van Berkel, S. P. Pasilis and O. Ovchinnikova, *J. Mass Spectrom.*, 2008, **43**, 1161–1180.
30 R. B. Cody, J. A. Laramee and H. D. Durst, *Anal. Chem.*, 2005, **77**, 2297–2302.
31 M.-Z. Huang, C.-H. Yuan, S.-C. Cheng, Y.-T. Cho and J. Shiea, *Annu. Rev. Anal. Chem.*, 2010, **3**, 43–65.
32 R. G. Cooks, Z. Ouyang, Z. Takats and J. M. Wiseman, *Science*, 2006, **311**, 1566–1570.
33 L. A. Leuthold, J.-F. Mandscheff, M. Fathi, C. Giroud, M. Augsburger, E. Varesio and G. Hopfgartner, *Rapid Commun. Mass Spectrom.*, 2006, **20**, 103–110.
34 T. J. Kauppila, A. Flink, M. Haapala, U.-M. Laakkonen, L. Aalberg, R. A. Ketola and R. Kostiainen, *Forensic Sci. Int.*, 2011, **210**, 206–212.
35 T. J. Kauppila, V. Arvola, M. Haapala, J. Pól, L. Aalberg, V. Saarela, S. Franssila, T. Kotiaho and R. Kostiainen, *Rapid Commun. Mass Spectrom.*, 2008, **22**, 979–985.
36 R. R. Steiner and R. L. Larson, *J. Forensic Sci.*, 2009, **54**, 617–622.
37 N. Talaty, C. C. Mulligan, D. R. Justes, A. U. Jackson, R. J. Noll and R. G. Cooks, *Analyst*, 2008, **133**, 1532–1540.
38 R. A. Musah, M. A. Domin, R. B. Cody, A. D. Lesiak, A. John Dane and J. R. E. Shepard, *Rapid Commun. Mass Spectrom.*, 2012, **26**, 2335–2342.
39 R. A. Musah, M. A. Domin, M. A. Walling and J. R. E. Shepard, *Rapid Commun. Mass Spectrom.*, 2012, **26**, 1109–1114.
40 A. D. Lesiak, R. A. Musah, M. A. Domin and J. R. E. Shepard, *J. Forensic Sci.*, 2013, in press.
41 M. Higuchi and K. Saito, *Bunseki Kagaku*, 2012, **61**, 705–711.
42 S. J. B. Dunham, P. D. Hooker and R. M. Hyde, *Forensic Sci. Int.*, 2012, **223**, 241–244.
43 K. E. Vircks and C. C. Mulligan, *Rapid Commun. Mass Spectrom.*, 2012, **26**, 2665–2672.
44 J. K. Dalgleish, M. Wleklinski, J. T. Shelley, C. C. Mulligan, Z. Ouyang and R. Graham Cooks, *Rapid Commun. Mass Spectrom.*, 2013, **27**, 135–142.
45 J. T. Shelley and G. M. Hieftje, *Analyst*, 2010, **135**, 682–687.
46 S. E. Rodriguez-Cruz, *Rapid Commun. Mass Spectrom.*, 2006, **20**, 53–60.
47 I. Ojanperä, M. Kolmonen and A. Pelander, *Anal. Bioanal. Chem.*, 2012, **403**, 1203–1220.
48 E. Fornal, A. Stachniuk and A. Wojtyla, *J. Pharm. Biomed. Anal.*, 2013, **72**, 139–144.
49 A. H. Grange and G. W. Sovocool, *Rapid Commun. Mass Spectrom.*, 2011, **25**, 1271–1281.
50 A. T. Navare, J. G. Mayoral, M. Nouzova, F. G. Noriega and F. M. Fernández, *Anal. Bioanal. Chem.*, 2010, **398**, 3005–3013.
51 S. Yu, E. Crawford, J. Tice, B. Musselman and J.-T. Wu, *Anal. Chem.*, 2008, **81**, 193–202.
52 R. B. Cody, *Anal. Chem.*, 2008, **81**, 1101–1107.
53 T. M. Vail, P. R. Jones and O. D. Sparkman, *J. Anal. Toxicol.*, 2007, **31**, 304–312.
54 S. D. McDermott, J. D. Power, P. Kavanagh and J. O'Brien, *Forensic Sci. Int.*, 2011, **212**, 13–21.

